

Formation of Chiral Soliton Lattice

Tetsutaro Higaki^{a,b} Kohei Kamada^c Kentaro Nishimura^{d,b}

^a*Department of Physics, Keio University, 3-14-1 Hiyoshi, Yokohama, Kanagawa 223-8522, Japan*

^b*Research and Education Center for Natural Sciences, Keio University, 4-1-1 Hiyoshi, Yokohama, Kanagawa 223-8521, Japan*

^c*Research Center for the Early Universe (RESCEU), Graduate School of Science, The University of Tokyo, Hongo 7-3-1 Bunkyo-ku, Tokyo 113-0033, Japan*

^d*KEK Theory Center, Tsukuba 305-0801, Japan*

E-mail: thigaki@rk.phys.keio.ac.jp, kohei.kamada@resceu.s.u-tokyo.ac.jp,
nishiken@post.kek.jp

ABSTRACT: The Chiral Soliton Lattice (CSL) is a lattice structure composed of domain walls aligned in parallel at equal intervals, which is energetically stable in the presence of a background magnetic field and a finite (baryon) chemical potential due to the topological term originated from the chiral anomaly. We study its formation from the vacuum state, with describing the CSL as a layer of domain-wall disks surrounded by the vortex or string loop, based on the Nambu-Goto-type effective theory. We show that the domain wall nucleates via quantum tunneling when the magnetic field is strong enough. We evaluate its nucleation rate and determine the critical magnetic field strength with which the nucleation rate is no longer exponentially suppressed. We apply this analysis to the neutral pion in the two-flavor QCD as well as the axion-like particles (ALPs) with a finite (baryon) chemical potential under an external magnetic field. In the former case, even though the CSL state is more energetically stable than the vacuum state and the nucleation rate becomes larger for sufficiently strong magnetic field, it cannot be large enough so that the nucleation of the domain walls is not exponentially suppressed and promoted, without suffering from the tachyonic instability of the charged pion fluctuations. In the latter case, we confirm that the effective interaction of the ALPs generically includes the topological term required for the CSL state to be energetically favored. We show that the ALP CSL formation is promoted if the magnetic field strength and the chemical potential of the system is slightly larger than the scale of the axion decay constant.

Contents

1	Introduction	1
2	Nucleation rate of the chiral soliton lattice	3
2.1	Chiral Soliton Lattice (CSL)	3
2.2	Nambu-Goto action for the wall-string system	6
2.3	Calculation of the decay rate	8
2.3.1	Nucleation of a single domain wall disk from the vacuum	8
2.3.2	Simultaneously generated domain walls and effects of background domain walls	11
3	Implication for physical specific systems	13
3.1	QCD	13
3.2	Axion Like Particle	14
4	Conclusion and Discussion	16

1 Introduction

The domain wall is a field configuration connecting two vacua and is identified as a two-dimensional topological defect. If the system has a periodic potential with (infinite) degenerate vacua, which typically appears for the pseudo Nambu-Goldstone bosons (pNGBs) associated with the spontaneous breaking of a global $U(1)$ symmetry, it allows a stack of parallel domain walls, well-known as the chiral soliton lattice (CSL). This state universally appears from condensed matter physics to high-energy physics. The CSL-type magnetic structure has been originally studied in chiral magnets [1] and experimentally observed [2] (see ref. [3] for review). In high energy physics, it has been shown, based on a low-energy effective theory that takes into account the chiral anomaly [4, 5], that the ground state of QCD at finite baryon chemical potential μ_B under a sufficiently strong magnetic field is the CSL of π_0 meson [5–7] (see also refs. [8–14] for related works). As other examples, the rotation-induced CSL [15–18], Floquet-engineered CSL [19], the CSL in QCD-like theory [20, 21], and the CSL-like pattern formation via nonequilibrium process [22] have also been discussed.

There are three important elements in theories that have the CSL state as the ground state, i) a pNGB (referring to ϕ) associated with the spontaneous breaking of a global symmetry G , ii) an explicit breaking of the symmetry G which leads to a periodic cosine-type potential, and iii) a total derivative term of ϕ .¹ With these ingredients, the low energy effective theory for the pNGB becomes the Sine-Gordon theory with the total derivative term. In the usual Sine-Gordon theory, the domain wall interpolating between the minima of the cosine-type potential appears. Such a field configuration is topologically protected, but energetically unfavorable compared to the trivial vacuum state. The

¹In the main text, we suppose that the origin of the total derivative term is the Chiral Separation Effect (CSE) [4, 23–25], but it does not always have to be the case. Depending on the underlying physics of the system, the origin of the total derivative term varies. For example, the Chiral Vortical Effect [26–31] leads to a rotational counterpart of the total derivative term discussed in refs. [15, 16]. In chiral magnets, the total derivative term of the magnon originates from the so-called Dzyaloshinskii-Moriya (DM) interaction [32, 33].

total derivative term decreases the tension of the domain wall, and it can be negative for a sufficiently large external background field. Consequently, the domain wall is energetically more favorable than the vacuum state.

A fact that a field configuration is energetically favorable does not mean that such a configuration is formed instantaneously. Noting that the domain walls are topologically stable, we expect that the CSL form with a non-trivial dynamics associated with a change of topological numbers. The first way to form the CSL that one can imagine would be the Kibble-Zurek mechanism [34, 35]. However, it requires the symmetry restoration with *e.g.*, a high-temperature environment and does not describe the defect formation from the vacuum state. In order to see the CSL formation at zero-temperature, we need to describe it as a quantum tunneling, which we would like to explore in the present paper.² Generally, it is difficult to calculate the nucleation rate of topological defects starting from the infinite dimensional quantum field theory. However, in ref. [37] a genius way to calculate it by describing the system in terms of the Nambu-Goto (NG) theory so that the problem becomes one-dimensional quantum mechanics has been proposed. Although this method was originally invented for the quantum creation of the topological defects in the (quasi) de Sitter background, it has been noticed that it can be useful for other phenomena such as the Schwinger effect or the vacuum decay through the bubble nucleation [38, 39]. In this paper, with adopting this method, we evaluate the single domain wall as well as the CSL formation rate. Noting that the formation of a domain wall spread to the spatial infinite would be unlikely to occur from the viewpoint of causality, we describe the system as a domain-wall disk surrounded by a vortex or string loop. The dynamics of the domain-wall disk can be then described by quantum mechanics for the radius of the disk, R . We show that when the tension of the domain wall is negative, the domain-wall disk with the radius R_2 (see eq. (2.34)) nucleates via quantum tunneling whose rate depends on the external magnetic field strength as well as the chemical potential of the system. We find that the nucleation rate is exponentially suppressed below the critical magnetic field amplitude B_c (see eq. (2.39)). Therefore, we emphasize that, even when the CSL state is more energetically favorable than the vacuum, the formation of the domain wall is not promoted instantaneously as long as $B < B_c$.

As concrete examples, we consider the following two realistic physical systems to which the effective theory is expected to be applied, namely, i) the neutral pion in the two-flavor Quantum Chromo Dynamics (QCD) and ii) Axion-Like Particles (ALPs) [40–46] at a finite chemical potential under an external magnetic field. In the former case, the properties of the CSL composed of the π_0 meson associated with the spontaneous chiral symmetry breaking have been studied in ref. [6]. There it has been pointed out that a too strong magnetic field causes a tachyonic instability of the charged pion fluctuation, which determines the upper bound of the magnetic field strength for the CSL. We find that the pion domain-wall as well as the pion CSL formation rate becomes larger for stronger magnetic fields, but at the upper bound of the magnetic field strength suggested by the stability against the charged pion fluctuation the formation rate is still exponentially suppressed even though the CSL state is more energetically favorable than the QCD vacuum. In the latter case with an ALP, we find for the first time that the total derivative term required for the CSL appears in the effective field theory from the Chiral Magnetic Effect (CME) [23, 25] and the CSL is a ground state for a sufficiently large external magnetic field. Compared to the case of the neutral pion, we do not have to worry about the instability of associated fields in the ALP sector if they are sufficiently heavy, if any. As a result, there will be no exponential suppression factor in the nucleation rate if the magnetic field and the chemical potential is slightly larger than the axion decay constant.

²See also ref. [36] for the phenomenological study on the CSL formation in the chiral magnets.

This paper is organized as follows. In the next section, we review the CSL and describe it in terms of the NG-type action. Then we estimate the formation rate of a single domain-wall as well as the CSL. In Sec. 3, we apply the results of Sec. 2 to the physically well-motivated system, that is, the neutral pion in the two-flavor QCD and the ALP. Sec. 4 is devoted for the conclusion and discussion.

2 Nucleation rate of the chiral soliton lattice

This section considers the nucleation of the CSL. Since the CSL is a topological defect, it is topologically distinct with the trivial field configuration and can be generated by the Kibble-Zurek mechanism [34, 35] or through quantum tunneling. Here we are interested in its nucleation at zero temperature, we shall study the latter. While a quantum field theoretic investigation is quite involved, here we adopt a quantum mechanical approach where the CSL is described by the Nambu-Goto-type action with a one dimensional parameter, that is, the radius of the wall, as has been first studied in ref. [37] and also recently adopted in refs. [38, 39]. In the following, we first review the nature of the CSL and develop its description by the Nambu-Goto-type action. Then we evaluate the nucleation rate for the single disk and the CSL.

2.1 Chiral Soliton Lattice (CSL)

We start with reviewing the CSL with a simple toy model. We consider a system in the uniform background magnetic field \mathbf{B} with the spontaneous chiral symmetry breaking whose low-energy dynamics can be described by the effective field theory of pNGB ϕ , which will be identified as a neutral pion or an ALP. Hereafter we neglect fields other than pNGB that may exist in theories of our interest unless otherwise stated, since they are supposed not to be directly associated with the CSL. For instance, we focus on a situation in which they are much heavier than pNGB. The effective Lagrangian of the pNGB up to the leading order is that of the Sine-Gordon theory, given by

$$\mathcal{L} = \frac{f^2}{2}(\partial_\mu\phi)^2 + f^2m^2(\cos\phi - 1) + \frac{\mu}{4\pi^2}\mathbf{B} \cdot \nabla\phi, \quad (2.1)$$

where f and m are the decay constant and the mass of the pNGB, respectively. The first term is the kinetic term, and the second is the potential associated with the explicit chiral symmetry breaking. The constant f^2m^2 is an offset to zero the energy of the vacuum at $\phi = 0$. The third term is introduced, for example, in the following reason. Here we suppose a system with N_f species of massless U(1) charged Dirac fermions ψ_i with their chemical potentials μ being coupled to the conserved charge $j^0 \equiv \sum_i^{N_f} \bar{\psi}_i \gamma^0 \psi_i$. This system exhibits the so-called chiral separation effect (CSE), where the axial vector currents $\mathbf{j}_5 \equiv \sum_i^{N_f} \bar{\psi}_i \gamma^5 \boldsymbol{\gamma} \psi_i$ are induced in the direction of the magnetic field as [4, 23–25]

$$\mathbf{j}_5 = \frac{\mu}{2\pi^2} \mathbf{B}, \quad (2.2)$$

where the gauge coupling is absorbed by the magnetic field. We shall note that this transport phenomenon is related to the chiral anomaly [25, 31, 47] and does not receive any renormalization. Hence, the CSE appears independently of the energy scale. In particular, in phases where the chiral symmetry is spontaneously broken, the anomaly matching condition tells that the CSE should be reproduced by the effective interaction of the resultant pNGBs, such as the mesons and axions, which leads to the third term in eq. (2.1). Note that under the chiral transformation $\psi \rightarrow e^{i\gamma^5\theta}\psi$ the NGB in the low energy effective theory transforms as $\phi \rightarrow \phi + 2\theta$.

Under the chiral rotation with a position-dependent $\theta = \theta(x)$, the action changes as $\delta S = \int d^4x (\partial_\mu \theta(x)) j_5^\mu = \frac{1}{2} \int d^4x (\partial_\mu \delta\phi) j_5^\mu$ from the Noether's theorem. Thus, we have $S = \frac{1}{2} \int d^4x (\partial_\mu \phi) j_5^\mu$ in the low energy regime.

The effective Hamiltonian coming from eq. (2.1) is now given as,

$$\mathcal{H} = \frac{f^2}{2} [(\partial_t \phi)^2 + (\partial_x \phi)^2 + (\partial_y \phi)^2 + (\partial_z \phi)^2] + f^2 m^2 (1 - \cos \phi) - \frac{\mu}{4\pi^2} B \partial_z \phi, \quad (2.3)$$

where we have set $\mathbf{B} = (0, 0, B)$ without loss of generality. In order to minimize the Hamiltonian, ϕ should not depend on t , x and y so that it becomes

$$\mathcal{H} = \frac{f^2}{2} (\partial_z \phi)^2 + f^2 m^2 (1 - \cos \phi) - \frac{\mu}{4\pi^2} B \partial_z \phi. \quad (2.4)$$

Note that in the equation of motion,

$$\partial_z^2 \phi = m^2 \sin \phi, \quad (2.5)$$

the topological term does not appear. Its solution with the boundary condition $\phi(-\infty) = 0$, $\phi(\infty) = 2\pi$ is the so-called domain wall:

$$\phi_{\text{DW}}(mz) = 4 \arctan[\exp(mz)]. \quad (2.6)$$

Substituting eq. (2.6) into eq. (2.4), the energy of this single soliton per unit area in the x - y plane can be calculated as

$$\mathcal{E}_{\text{DW}} \equiv \int_{-\infty}^{\infty} dz \mathcal{H}[\phi_{\text{DW}}(z)] = 8mf^2 - \frac{\mu B}{2\pi}. \quad (2.7)$$

We can see that while the topological term does not appear in the equation of motion, it appears in the energy. In the absence of topological term, the energy of this single domain wall is, of course, larger than the vacuum energy 0 (or the energy of the trivial configuration $\phi = 0$). On the other hand, as the magnetic field B increases and exceeds the critical magnetic field,

$$B_{\text{DW}} = \frac{16\pi m f^2}{\mu}, \quad (2.8)$$

the sign of \mathcal{E}_1 changes from positive to negative. In such a case, the domain wall is not only topologically stable but also energetically favorable, which opens up the possibility to form it as a quantum vacuum decay.

The fact that the single domain wall is more stable than the vacuum state $\phi = 0$ tells that the ground state of the system at $B > B_{\text{DW}}$ would be a parallel stack of this domain walls. Since the wall-wall interaction would generate a positive energy, there should be an appropriate distance between the walls to minimize the energy. The configuration of such a state, called the chiral soliton lattice (CSL), is determined as follows. One of the general solutions of eq. (2.5) that satisfies $\phi(0) = -\pi$ is given as

$$\int_0^{\phi/2 + \pi/2} d\theta \frac{1}{\sqrt{1 - k^2 \sin^2 \theta}} = \frac{zm}{k}. \quad (2.9)$$

Note that both sides of the equation above are zero when $\phi = -\pi$ and $z = 0$, and the solution is a function of zm/k , with k ($0 < k < 1$) being the parameter that characterizes the solution. In terms of the Jacobi's amplitude function am , it is rewritten as

$$\frac{1}{2} \left(\phi_k \left(\frac{zm}{k} \right) + \pi \right) = \text{am} \left(\frac{zm}{k}, k \right). \quad (2.10)$$

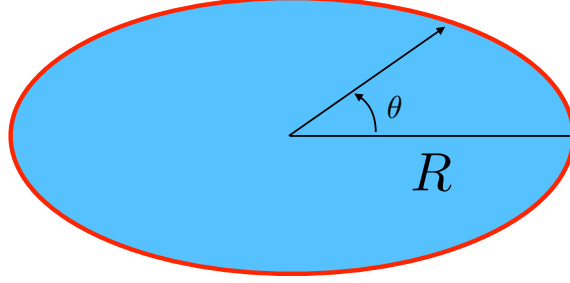


Figure 1. Schematic picture of the domain wall disc with the string on the edge. The blue part corresponds to the domain wall, the red the string. The parameter θ parametrizes the string on the edge of the wall.

Equivalently, ϕ is also given by the Jacobi's elliptic function:

$$\cos\left(\frac{1}{2}\phi_k\left(\frac{zm}{k}\right)\right) = \operatorname{sn}\left(\frac{zm}{k}, k\right). \quad (2.11)$$

In the equations above, it has been assumed that $\partial_z\phi > 0$ and $\mu B > 0$ without a loss of generality, such that $\mu B\partial_z\phi > 0$.³ Note that the parameter k is now identified as the elliptic modulus. Using the complete elliptic integral of the first kind $K(k)$, the periodicity of this solution is given by

$$l = \frac{2kK(k)}{m}, \quad \text{where} \quad 2K(k) = \int_0^\pi d\theta \frac{1}{\sqrt{1 - k^2\sin^2\theta}}, \quad (2.12)$$

with shifts of $\Delta\phi = 2\pi$ and $\Delta z = l$, which corresponds to the distance between the walls. The minimization of the energy of each wall with period $l = l(k)$ per unit area in the xy plane,

$$\mathcal{E}_{\text{CSL}} \equiv \int_{-l(k)/2}^{l(k)/2} dz \mathcal{H}[\phi_k(z)] = 4mf^2 \left[\frac{2E(k)}{k} + \left(k - \frac{1}{k}\right) K(k) \right] - \frac{\mu B}{2\pi}, \quad (2.13)$$

optimizes the free parameter k for given parameters, μ, B, m, f . The optimal condition is given by [6]

$$\frac{E(k)}{k} = \frac{\mu B}{16\pi m f^2}, \quad (2.14)$$

where $E(k)$ is the complete elliptic integral of the second kind, which determines the elliptic modulus for the CSL, $k = k_{\text{CSL}}$, and hence the wall distance l for given parameters, μ, B, m, f . Note that its left-hand side is bounded from below as $E(k)/k > 1$ ($0 < k < 1$). Not the vacuum solution but the CSL is the ground state if eq. (2.14) has a solution for $0 < k < 1$, and hence the critical magnetic field strength for the CSL to be the ground state, B_{CSL} , is equal to eq. (2.8),

$$B_{\text{CSL}} = B_{\text{DW}} = \frac{16\pi m f^2}{\mu}. \quad (2.15)$$

In a large magnetic field limit of $B \gg B_{\text{CSL}}$ ($k \rightarrow 0$), in which pNGB mass is neglected, the solution minimizing the Hamiltonian is given by

$$\phi(z) \simeq \frac{\mu B z}{4\pi^2 f^2}. \quad (2.16)$$

Then, the period reads

$$l \simeq \frac{8\pi^3 f^2}{\mu B}. \quad (2.17)$$

³Instead, a solution is given by $\frac{1}{2}(\phi_k(\frac{zm}{k}) + \pi) = -\operatorname{am}(\frac{zm}{k}, k)$ when $\partial_z\phi < 0$ and $\mu B < 0$.

2.2 Nambu-Goto action for the wall-string system

We have reviewed that the ground state of the Sine-Gordon theory becomes the CSL state due to the topological term. This suggests that the CSL with finite topological numbers can be formed from the vacuum state. Here, we argue the domain wall formation through the quantum-mechanical tunneling. It is easy to imagine that not the infinite domain wall in x - y plane is generated instantaneously but a disk-like domain wall with a finite size surrounded by a vortex or a string loop [48–50], as shown in Fig. 1, is generated first and eventually expands. Such a system can be formed through spontaneous breaking of the chiral symmetry in the QCD [48–50] or a that of $U(1)_{\text{PQ}}$ in models with ALPs [51–53]. Infinite dimensional quantum field theoretic approach on the formation of such a field configuration is quite involved, and hence we adopt the thin-wall approximation so that the field configuration can be described by one-dimensional Nambu-Goto-like action as has been studied in refs. [37–39]. In this subsection, we construct this one-dimensional effective action for the wall-string system.

Here we consider the wall-string system in the Minkowski background,

$$ds^2 = \eta_{\mu\nu} dx^\mu dx^\nu = -dt^2 + d\Omega_3, \quad (2.18)$$

where $d\Omega_3$ is the line element on the three-dimensional Euclidean space. The Nambu-Goto like effective action [54] of the domain-wall disk surrounded by an edge can be divided into the wall (void) part and string (edge) part as

$$S = S_{\text{wall}} + S_{\text{string}} = -\sigma \int_{\mathcal{W}} d^3\zeta \sqrt{\det h_{ab}} - T \int_{\partial\mathcal{W}} d^2\xi \sqrt{-\det\gamma_{\alpha\beta}}, \quad (2.19)$$

where σ and T are the wall and string tensions, h_{ab} and $\gamma_{\alpha\beta}$ are the induced metrics on the three-dimensional world volume for the wall and two-dimensional world sheet for the string, respectively.

Let us first investigate the former, the wall action. The induced metric on the wall is given by

$$h_{ab} = \eta_{\mu\nu} \frac{\partial X^\mu}{\partial \zeta^a} \frac{\partial X^\nu}{\partial \zeta^b}, \quad (2.20)$$

where $X^\mu(\zeta)$ is the three-dimensional world volume of the domain wall embedded in the bulk spacetime, \mathcal{W} , with ζ^a ($a = 0, 1, 2$) being the coordinate covering \mathcal{W} . Here ζ^0 is chosen to be timelike whereas $\zeta^{1,2}$ are chosen to be spacelike. Since we are interested in the disk-like configuration where the wall is perpendicular to the z axis while rotational symmetric in the x - y plane, it is natural to take the coordinate on the wall to be $\{\zeta^a\} = \{\tau, \chi, \theta\}$ and the trajectory to be $\{X^\mu\} = \{t(\zeta), r(\zeta), \Theta(\zeta), z = z_0\}$. Fixing the gauge as $\tau = t$, $\chi = r$, and $\theta = \Theta$, the induced metric is given as

$$h_{ab} = \text{diag}(1, -1, -r^2), \quad (2.21)$$

where we have taken the cylindrical coordinate system for the background Minkowski metric, $ds^2 = dt^2 - dr^2 - r^2 d\theta^2 - dz^2$. The tension of the wall is calculated by integrating the energy density along the z -axis. For the single domain wall solution eq. (2.6), we obtain

$$\sigma \equiv \int dz \mathcal{H} = 8mf^2 - \frac{\mu B}{2\pi}. \quad (2.22)$$

Note that the tension is negative at $B > B_{\text{DW}} = B_{\text{CSL}}$. Since we consider the case where the disk radius can change with time, the domain of r is given as $0 < r < R(\tau)$. Consequently, we get the Nambu-Goto-like action for the domain-wall disk as

$$S_{\text{wall}} = -\sigma \int_{\mathcal{W}} d^3\zeta \sqrt{\det h_{ab}} = -\sigma \int d\tau \int_0^{R(\tau)} dr \int_0^{2\pi} d\theta r = -\pi\sigma \int d\tau R(\tau)^2. \quad (2.23)$$

Similarly to the wall part, the induced metric on the string worldsheet is given by

$$\gamma_{\alpha\beta} = \eta_{\mu\nu} \frac{\partial X^\mu}{\partial \xi^\alpha} \frac{\partial X^\nu}{\partial \xi^\beta}, \quad (2.24)$$

where $X^\mu = X^\mu(\xi)$ describes the two-dimensional string worldsheet $\partial\mathcal{W}$ with the radius R embedded in the bulk spacetime as shown in Fig. 1 so that we can take $\{X^\mu\} = \{t(\xi), R(t(\xi)), \Theta(\xi), z = z_0\}$, with ξ^α ($\alpha = 0, 1$) being the coordinate covering the $\partial\mathcal{W}$, $\{\xi^a\} = \{\tau, \theta\}$. We gauge-fix the coordinates as $\tau = t$ and $\theta = \Theta$, and emphasize that R is a dynamical and depends on t : $R = R(t) = R(\tau)$ on the $\partial\mathcal{W}$. Then, its explicit form is calculated as

$$\gamma_{\alpha\beta} = \text{diag}(1 - \dot{R}^2, -R^2), \quad (2.25)$$

or

$$ds_{\text{worldsheet}}^2 = (1 - \dot{R}^2)d\tau^2 - R^2d\theta^2, \quad (2.26)$$

where the dot represents the derivative with respect to τ . The string action is proportional to the worldsheet area:

$$S_{\text{string}} = -T \int d\tau d\theta \sqrt{-\gamma} = -2\pi T \int d\tau R \sqrt{1 - \dot{R}^2}, \quad (2.27)$$

where the string tension evaluated at far from the string core, T , is the summation of the potential energy and the gradient energy of the radial direction of the symmetry breaking field or the order parameter and is calculated as [55, 56]

$$T \sim 2\pi \times 2f^2 \times \ln \frac{R_c}{r_c}, \quad (2.28)$$

where R_c and $r_c \sim f^{-1}$ are cutoff length and string core size, respectively. Here we have only taken into account the classical contribution from the radial direction of the symmetry breaking field that does not couple to the magnetic field. Thus we regard that the string tension is independent of the magnetic field throughout this paper. Once we take into account light matter fields charged under the U(1) gauge theory, however, there can arise a magnetic-field-dependent contribution to the string tension through, e.g., the fermion zero modes, but it is UV model-dependent. Since the classical part would generally dominate over the whole contribution in the tension, we expect that our analysis would be valid, even if the string tension is affected by the magnetic field, depending on the detail of the model. The potential energy stored inside of the core is estimated as of order f^2 , whereas the gradient energy gives the logarithmic factor. A naive choice of R_c would be the disk radius R_d . However, in the wall-string system the field configuration around the string is non-trivial and different from the string without being attached to a wall, and hence careful numerical study is needed for the estimate for the cutoff length or the gradient energy. Instead, here we take R_c as a parameter independent of the disk radius R_d throughout this paper, leaving its precise determination for future study. In ref. [57], the authors have numerically shown $T \sim f^2 \sim \text{const.}$, independent of the disk radius as well as the magnetic field strength, at a distance from a domain wall disk bounded by a string loop. That is because unlike the strings without being attached to a wall, the field configuration appears to exponentially come close to that of the vacuum, in which there exists no solitons, as being away from such a disk, regardless of the value of the wall radius. In this case, one length scale that could be related to the string configuration is the thickness of the wall, $r_w \sim 1/m$. Hence another plausible estimate for R_c would be the thickness of the wall, r_w , which is independent of R_d , but careful investigations are needed to confirm this ansatz. ⁴

⁴We thank M. Eto and M. Nitta for pointing out this fact.

2.3 Calculation of the decay rate

Now we are ready to evaluate the quantum mechanical disk nucleation rate with the help of the Nambu-Goto-like effective action. As we have discussed the field configurations for the single domain-wall disk and the CSL-like disk layer are different, we need carefully to take care of the difference. We will first examine the single disk nucleation and then discuss the CSL formation.

2.3.1 Nucleation of a single domain wall disk from the vacuum

First we consider the tunneling process where a single wall is created from the vacuum. From the discussion in the previous section, the dynamics of a single domain-wall disk is described by one-dimensional quantum mechanics of the disk radius $R(\tau)$ with the effective action,

$$S_{\text{tot}} = S_{\text{wall}} + S_{\text{string}} = -\pi \int d\tau \left(2TR\sqrt{1 - \dot{R}^2} + \sigma R^2 \right). \quad (2.29)$$

In order to study the dynamics of this domain wall system, it is convenient to use the conserved energy,

$$E = p\dot{R} - L, \quad (2.30)$$

where the Lagrangian L can be read from the action S_{tot} , $L = -\pi(2TR\sqrt{1 - \dot{R}^2} + \sigma R^2)$, and p is the momentum conjugate to R ,

$$p = \frac{\partial L}{\partial \dot{R}} = \frac{2\pi TR\dot{R}}{\sqrt{1 - \dot{R}^2}}. \quad (2.31)$$

The conservation law can be rewritten as the following form,

$$\dot{R}^2 + \left[\frac{R^2}{\left(\epsilon - \frac{\sigma R^2}{2T}\right)^2} - 1 \right] \equiv \dot{R}^2 + 2V(R) = 0, \quad (2.32)$$

where we have introduced $\epsilon = E/(2\pi T)$. The first and second terms can be identified as the kinetic and potential terms of $R(t)$, respectively. Note that $V(R)$ diverges for $\sigma > 0$ at $R = R_{\text{div}} \equiv \sqrt{2\epsilon T/\sigma}$ with $R_1 < R_{\text{div}} < R_2$ and hence nucleation rate is expected to be highly suppressed. We can see that for $T > -2\epsilon\sigma$ or $T^2 > -\sigma E/\pi$ this potential has a potential barrier between $R = 0$ and ∞ as shown in Fig. 2. Note that for $\sigma < 0$, the barrier height is finite and hence it is possible for the quantum tunneling to happen. By solving $V(R) > 0$ we find the starting and end points, R_1 and R_2 as

$$R_1 = \begin{cases} \frac{T}{\sigma} \left[-1 + \sqrt{1 + 2\epsilon\sigma/T} \right] & (\epsilon > 0) \\ \frac{T}{\sigma} \left[1 - \sqrt{1 + 2\epsilon\sigma/T} \right] & (\epsilon < 0) \end{cases}, \quad R_2 = \frac{T}{\sigma} \left[-1 - \sqrt{1 + 2\epsilon\sigma/T} \right], \quad (2.33)$$

where we have taken $\sigma < 0$, which corresponds to take $B > B_{\text{DW}}$. The structure of the potential tells that the disk radius R can change classically at $0 < R < R_1$ and $R > R_2$. If the initial disk radius is at $0 < R < R_1$, it can expand up to $R = R_1$ and then recollapses to $R = 0$. On the other hand, for the initial condition $R > R_2$, the disk radius expands towards infinity.

Although the classical dynamics is forbidden in the range $R_1 < R < R_2$, the domain wall disk can nucleate by the quantum tunneling through the potential barrier. The tunneling probability from $R = R_1$ to $R = R_2$ can be evaluated as follows [58]. By performing a Wick rotation, $\tau \rightarrow -i\tau_E$, we obtain the Euclidean action,

$$S_E[R] = \pi \int d\tau_E \left(2TR\sqrt{1 + \left(\frac{dR}{d\tau_E}\right)^2} + \sigma R^2 \right). \quad (2.34)$$

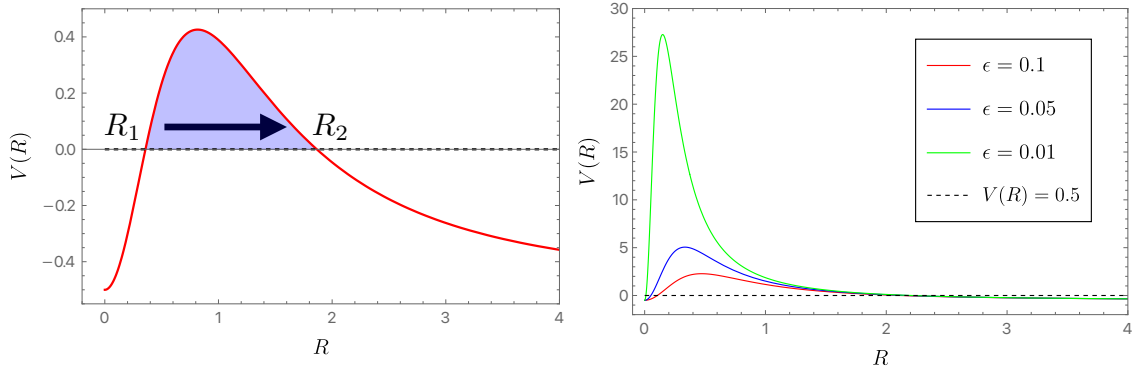


Figure 2. (*Left panel*) Typical shape of the potential $V(R)$ as a function of R is shown in the solid red line ($\sigma/T = -0.9$ and $\epsilon = 0.3$). For $\sigma < 0$ the barrier height is finite. The black dotted one represents the line for $V(R) = 0$. $V(R)$ is positive in the blue region at $R_1 < R < R_2$, in which region classical dynamics is forbidden. (*Right panel*) ϵ -dependence of the shape of the potential $V(R)$ for $\sigma/T = -0.9$ is shown. The potential barrier tends to be higher for smaller ϵ , while the width of barrier $\Delta R \equiv R_2 - R_1 \sim R_2 \sim -2T/\sigma$ is insensitive to ϵ .

The bounce solution for the Euclidean action satisfies the conservation law with the flipped potential as

$$\left(\frac{dR}{d\tau_E}\right)^2 - 2V(R) = 0, \quad (2.35)$$

with the boundary condition $V(R_1) = V(R_2) = 0$. With this solution, we can evaluate the bounce action. Since we are interested in the domain-wall disk nucleation from the nothing, we take the limit $\epsilon \rightarrow +0$ so that

$$R_1 = 0, \quad R_2 = -\frac{2T}{\sigma}. \quad (2.36)$$

As for the sign of a small ϵ , note that the conserved energy is approximately given by the rest energy of a contribution of the string tension plus the wall tension, $E \simeq 2\pi RT + \pi R^2 \sigma = |\sigma| \pi R (R_2 - R)$, when the kinetic energy (expansion of the radius) is small. As long as we focus on the tunneling process between $R = 0$ and $R = R_2$, $E \propto \epsilon$ is necessarily positive because the positive string tension dominates over the conserved energy in the range of such a small R . (A large wall with $R > R_2$ cancels also the kinetic energy such that $E \propto \epsilon = 0$ owing to the negative tension.) See Fig. 2 to show this tendency. Note that the zero initial radius of the domain-wall disk means that there was no domain wall at all. By solving the bounce equation for $\epsilon \rightarrow 0$ and changing the variables from the Euclidean time τ_E to the disk radius R , the bounce action is evaluated as

$$\mathcal{B} = 2 \times 2\pi T \int_0^{R_2} dR \sqrt{R^2 - (\sigma R^2/2T)^2} = \frac{16\pi T^3}{3\sigma^2}, \quad (2.37)$$

where the factor 2 comes from the bounce trajectory, $R : 0 \rightarrow R_2 \rightarrow 0$. We can see that the tunneling action \mathcal{B} remains finite in the limit of $\epsilon \rightarrow 0$. Consequently, the nucleation rate P that the domain-wall disk with the radius $R = R_2 = -2T/\sigma$ nucleates is given by

$$P \simeq \mathcal{A} e^{-\mathcal{B}} = \mathcal{A} e^{-16\pi T^3/3\sigma^2}, \quad (2.38)$$

where the prefactor \mathcal{A} counts for the effects of quantum fluctuation around the bounce solution [37, 58, 59].

While the domain-wall disk nucleation rate is exponentially suppressed for $\mathcal{B} \gg 1$, it is unsuppressed for $\mathcal{B} \lesssim 1$. Noting that $T \simeq 4\pi f^2 \ln(R_c/r_c)$ and $\sigma \simeq 8mf^2 - \mu B/2\pi$, we find that for a sufficiently large magnetic field,

$$B > B_c = \frac{16\pi m f^2}{\mu} \left(\frac{(\ln(R_c/r_c))^{3/2}}{\sqrt{3}} \frac{4\pi^2 f}{m} + 1 \right) (> B_{\text{DW}}), \quad (2.39)$$

the nucleation rate is unsuppressed, which is the main result of the present paper.

The prefactor \mathcal{A} can, in principle, be calculated by evaluating the quantum fluctuations around the saddle point solution, but the calculation is rather involved in practice. Instead here we resort to the dimensional analysis. The action of the domain-wall disk bounded by the string has the time transitional symmetry, and hence the wall production can happen anytime. The zero mode corresponding to the time-translation symmetry gives a contribution $\mathcal{T} \sqrt{\mathcal{B}/(2\pi)}$ to \mathcal{A} . As with time translational symmetry, the action also has the spatial translational symmetry so that the wall disk production can occur anywhere. Thus there appears a contribution of $V(\sqrt{\mathcal{B}/(2\pi)})^3$ in \mathcal{A} . Taking into account the characteristic length scale of the domain-wall disk, $R_d = R_2 = |2T/\sigma|$, we estimate \mathcal{A} as

$$\mathcal{A} \propto \left(\frac{\mathcal{B}}{2\pi} \right)^2 \frac{1}{R_d^4}. \quad (2.40)$$

Before proceeding, let us comment on the assumption we have made. In the above discussion, we have assumed that the system is well described by the domain-wall disk surrounded by the string. In other words, we have assumed that the thickness of the wall r_w and the radius of the string r_c are infinitely thin. The former is evaluated as $r_w \sim 1/m$ while the latter is evaluated as $r_c \sim 1/f$. The thin-wall/string approximation is valid if they are smaller than the disk radius R_d . Noting that $R_d = 2T/|\sigma|$, the conditions read

$$\frac{r_c}{R_d} \sim \frac{1/f}{2 \times 4\pi f^2 \ln(R_c/r_c)/(8mf^2|1 - B/B_{\text{DW}}|)} \sim \frac{m}{\pi f \ln(R_c/r_c)} \left(\frac{B}{B_{\text{DW}}} - 1 \right) \ll 1, \quad (2.41)$$

$$\frac{r_w}{R_d} \sim \frac{1/m}{2 \times 4\pi f^2 \ln(R_c/r_c)/(8mf^2|1 - B/B_{\text{DW}}|)} \sim \frac{1}{\pi \ln(R_c/r_c)} \left(\frac{B}{B_{\text{DW}}} - 1 \right) \ll 1. \quad (2.42)$$

With estimating the logarithmic factor with the cutoff length for the string to be of order of the unity, we find that the thin-wall approximation is valid for the magnetic field strength slightly larger than B_{DW} . Strictly speaking, the wall disk nucleation rate evaluated in the above cannot be used for much larger magnetic fields. In particular, the critical magnetic field for the bubble nucleation B_c (eq. (2.39)) is likely much larger than B_{DW} (for example, $B_c \sim (f/m)B_{\text{DW}} \gg B_{\text{DW}}$ for $f \gg m$). However, in ref. [39] where the three-dimensional bubble domain wall formation is studied with a Lorentzian formalism, the exponential suppression factor of the nucleation rate for a bubble with a larger radius is turned out to be the same to that for the critical bubble. This is understood that the classical expansion after the quantum tunneling to the critical bubble is evaluated in a completely quantum mechanical way. We expect the same argument follows so that our estimate of the bounce action for the critical disk (with $R_d = R_c$) gives that for the disk with larger radius, where the thin-wall approximation is better. Moreover, we do not expect that the nucleation rate for the disk wall with the radius smaller than the wall thickness is much more enhanced than the estimate in the above, since

the action of the field configuration of such thick wall disk would be the same order to the thin-wall approximation. Therefore we expect that the bounce action eq. (2.37) gives a good estimate for the suppression factor for the total wall disk nucleation rate even for the thin-wall approximation is not good for $R_d = R_c$.

2.3.2 Simultaneously generated domain walls and effects of background domain walls

Next we examine how the CSL forms. When multiple domain walls are simultaneously created from the vacuum and the CSL system is formed (see Fig. 3), a wall feels the existence of the neighbouring walls, and hence a nucleation rate of one of the walls would be affected. In order to take this effect into account, let us focus on a single wall which constitutes the CSL and consider its tunneling process. The critical difference to the single disk formation from the vacuum studied in Sec. 2.3.1 is the wall tension, because the wall feels the repulsive force originated from the other background walls. Let us remind that the wall tension for the domain wall layer (eq. (2.10)) is given by eq.(2.13),

$$\tilde{\sigma} = \mathcal{E}_{\text{CSL}} = 4mf^2 \left[\frac{2E(k)}{k} + \left(k - \frac{1}{k} \right) K(k) \right] - \frac{\mu B}{2\pi}, \quad (2.43)$$

and the minimization condition that optimizes the parameter $k = k_{\text{CSL}}$ is given by (2.14). We note

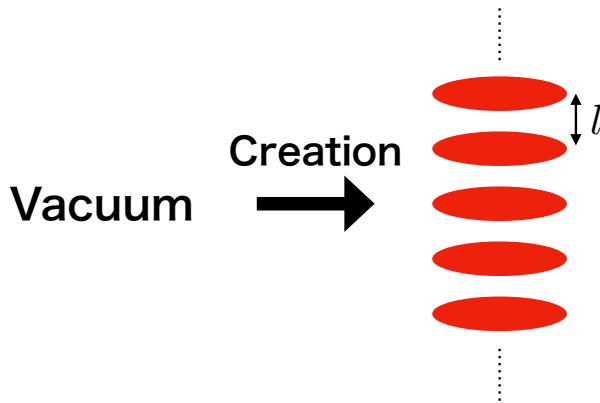


Figure 3. Schematic picture for the simultaneous nucleation of the domain walls at the interval l is shown. We note that l is the lattice space that minimizes the energy density of the domain wall [6].

that $\sigma < \tilde{\sigma} < 0$ is satisfied. ⁵This is because repulsive forces working between the walls increases the tension and hence an isolated wall is energetically more favorable. By replacing the wall tension σ by $\tilde{\sigma}$ in eq. (2.38), we obtain the wall disk nucleation rate, which is suppressed by the exponential factor $e^{-\mathcal{B}(\tilde{\sigma})}$, where $\mathcal{B}(\tilde{\sigma}) = 16\pi T^3/3\tilde{\sigma}^2$. Strictly speaking, this rate is those for a single disk nucleated at the deficit of the CSL with a distance of $2l(k_{\text{CSL}})$, we suppose it gives a good approximation for the CSL (with a finite boundary being surrounded by strings) formation rate itself. The B -dependence of \mathcal{B} is shown in Fig. 4. Note that the production of the domain wall is promoted when $\mathcal{B} \lesssim 1$ is satisfied. Supposing that $\ln(R_c/r_c)$ is order of the unity, we find that a single wall disk is easily nucleated for $B \gtrsim (10-20)B_{\text{DW}}$ while a fast CSL formation requires relatively larger magnetic fields, $B \gtrsim 10^3 B_{\text{DW}}$.

⁵The derivative of $\sigma - \tilde{\sigma}$ with respect to μB is $-E(k)/(4\pi K(k)) < 0$ and $\lim_{B \rightarrow B_c} \sigma - \tilde{\sigma} = 0$. Then, we get $\sigma < \tilde{\sigma}$. Even though the amplitude of $\tilde{\sigma}$ is smaller than σ , the number density of the wall in z -direction is larger, the total energy density in the whole space is smaller for the CSL state.

This is because the amplitude of the wall tension is smaller for the CSL than that of the single disk, which is energetically less favored. One may think that the nucleation rate would not be so suppressed compared to the one from the vacuum until the domain wall separation becomes comparable to the one for the CSL state. However, the nucleation rate strongly depends on the (absolute value of) domain wall tension. Since the interaction between the domain wall is always repulsive due to the gradient energy of the ϕ field, and hence the domain wall tension itself increases as we decrease the lattice separation ℓ with staying negative for $B > B_{\text{DW}}$. Note that even though the CSL state has larger tension, it is energetically favored, since the number density of the walls in z -direction is larger. As we have discussed in the previous subsection, for such strong magnetic fields, the thin-wall approximation does not hold for the disk with the critical radius $R = R_2 = 2T/|\tilde{\sigma}|$. However, the CSL with the infinite radius are formed through the expansion of the one with a finite radius, for which the thin-wall approximation holds at some point. Since the suppression factor of the nucleation rate of the wall disk with larger radius is expected to be the same, as has been studied in ref. [39], the estimate read from Fig. 4 would be appropriate to evaluate the disk/CSL formation rate.

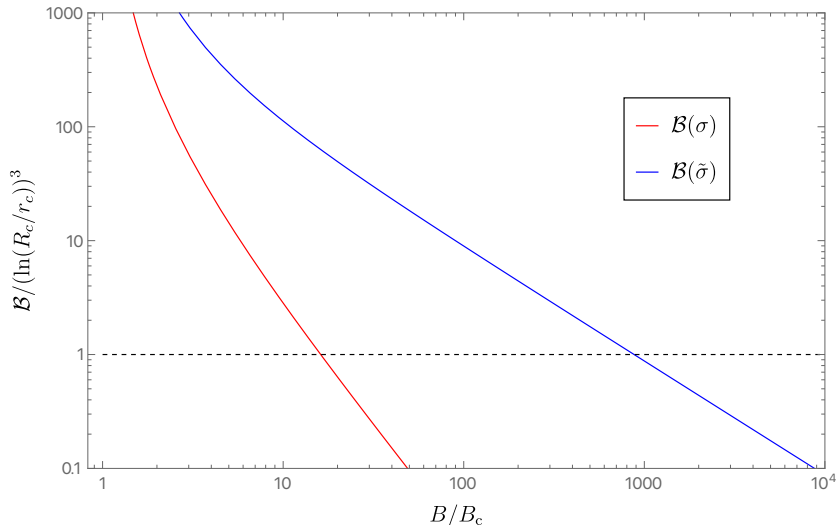


Figure 4. The B -dependence of the bounce action \mathcal{B} for the single disk (red line) and the CSL (blue line) is shown. Since $|\tilde{\sigma}|$ is smaller than $|\sigma|$, the bounce action for the single disk is smaller than that for the CSL. The black dotted line shows $\mathcal{B}/(\ln(R_c/r_c))^3 = 1$. We emphasize that the point where it intersects with the solid lines gives a critical magnetic field where the nucleation rate is no longer exponentially suppressed.

Before concluding this section, let us discuss how the system evolves as a whole. Once a single domain-wall disk forms quantum mechanically with a rate $\propto e^{-\mathcal{B}(\sigma)}$, it expands classically because the potential $V(R)$ monotonically decreases at $R > R_2$. If another disk has been created in the same x - y plane, the disks will eventually collide and merge each other. If $\mathcal{B}(\sigma) < 1$, the single wall production rate in a x - y plane is large and the radius of the domain wall becomes effectively infinite in the x - y plane quickly. If it is also the case with $\mathcal{B}(\tilde{\sigma}) < 1$, the domain wall formation in the z direction is not suppressed in spite of the repulsive force of the background walls [60] so that the CSL forms quickly with infinite in the x - y direction in a similar way to the ordinary liquid/gas transition (in 2-dimension). On the other hand, if $\mathcal{B}(\sigma) < 1 < \mathcal{B}(\tilde{\sigma})$, the completion of the CSL formation takes time while infinite domain walls with a relatively large distances are formed relatively quickly through the merger of the

disks in the same x - y plane. Even in the presence of disks, the nucleation rate in the same x - y plane is not suppressed compared to the one from the vacuum and they will merge relatively quickly to form the domain wall with an infinite radius. On the other hand, due to the repulsive force between walls in the z -direction, the nucleated domain walls are hard to merge into other walls along z -direction. Therefore, the bubble collision along z -direction is expected to be rare and hence the phase transition from the vacuum to the CSL is harder than that from the vacuum to a wall which is infinitely distant to other walls both in z - and x - y direction.

3 Implication for physical specific systems

The discussions in the previous section is based on a simple toy model only with a pNGB, which catches up the basic physics. Once we consider more realistic models, some of the details are different, such as the definition of μ and \mathbf{j}_5 , while quantitative arguments are possible. In this section, we take the neutral pion in QCD and axions in the early Universe as examples and discuss their phenomenology.

3.1 QCD

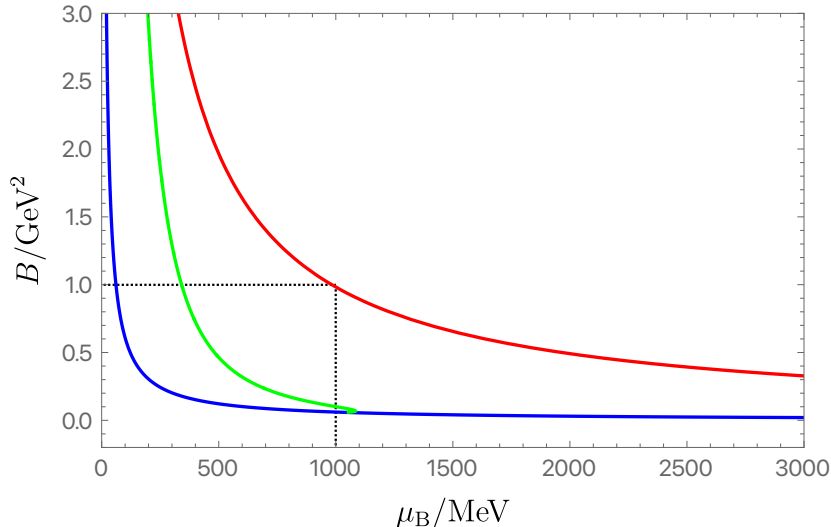


Figure 5. The critical magnetic fields for the state, $B_{\text{CSL}}^{\pi_0}$ (Blue), for the BEC, $B_{\text{BEC}}^{\pi_{\pm}}$ (Green), and for the single disk nucleation, $B_c^{\pi_0}$ (Red) are shown as functions of μ_B . The region below the blue line indicates the parameter space where the ground state is the QCD vacuum. The area between the blue and green line is the parameter space where the π_0 CSL state is the ground state, while in the region above the green line the CSL state is unstable and the ground state becomes π_{\pm} BEC state. In the region above the red line, the nucleation of the domain walls is promoted promptly without the exponential suppression. We emphasize, however, this region lies above the green line, where the CSL is no longer the vacuum state, as well as the black dotted line ($B = 1\text{GeV}^2$ and $\mu_B = 1\text{GeV}$), which indicates the boundary of the region where the chiral perturbation theory is valid.

Let us first apply our result to that in 2-flavor QCD at the finite baryon chemical potential μ_B under the external magnetic field, where the low energy effective theory is described by the neutral and charged pions. In this case, the relevant effective action for the CSL is described by eq. (2.1) just

by replacing μ with μ_B , ϕ with the neutral pion π , f with the pion decay constant f_π , and m with the pion mass m_π . From the same discussion in section 2.1, the CSL of the neutral pion becomes the ground state for the magnetic field larger than the critical magnetic field, $B_{\text{CSL}}^{\pi_0}$ (eq. (2.15)),

$$B_{\text{CSL}}^{\pi_0} = \frac{16\pi m_\pi f_\pi^2}{\mu_B}. \quad (3.1)$$

On the other hand, as pointed out in ref. [6], the charged pion fluctuations around the CSL state are tachyonic when the magnetic field strength is sufficiently large, $B > B_{\text{BEC}}^{\pi_\pm}$, with

$$B_{\text{BEC}}^{\pi_\pm} = \frac{m_\pi^2}{k^2} \left(2 - k^2 + 2\sqrt{1 - k^2 + k^4} \right), \quad (3.2)$$

where k is the elliptic modulus satisfying the following condition (see eq. (2.14)):

$$\frac{E(k)}{k} = \frac{\mu_B B_{\text{BEC}}^{\pi_\pm}}{16\pi m_\pi f_\pi^2}. \quad (3.3)$$

Eq. (3.3) determines k as a function of μ_B and $B_{\text{BEC}}^{\pi_\pm}$. Solving eq. (3.2) with this k , we can determine the μ dependence of $B_{\text{BEC}}^{\pi_\pm}$. It has been shown that $B_{\text{CSL}}^{\pi_0} < B_{\text{BEC}}^{\pi_\pm}$ for the parameter space of the interest [6], and hence the neutral pion CSL can exist stably for the magnetic fields in this range.

The question is now whether the CSL can form quickly via nucleation in this range of the magnetic fields. The critical magnetic field for the single wall disk formation (2.39) can be applied into this case by the replacement $m \rightarrow m_\pi$ and $f \rightarrow f_\pi$:

$$B_c^{\pi_0} = \frac{16\pi m_\pi f_\pi^2}{\mu_B} \left| \frac{(\ln(R_c/r_c))^{3/2}}{\sqrt{3}} \frac{4\pi^2 f_\pi}{m_\pi} + 1 \right|. \quad (3.4)$$

Figure 5 show these critical magnetic field strength as a function of μ_B , together with the lines $B = 1\text{GeV}^2$ and $\mu_B = 1\text{GeV}$, which indicates the upper bound of the validity of the effective theory described by pions [61, 62]. Here we take the physical values $f_\pi \approx 93\text{ MeV}$ and $m_\pi \approx 140\text{ MeV}$. We can see that $B_c^{\pi_0} > B_{\text{BEC}}^{\pi_\pm}$ is always satisfied. Moreover, in the parameter space with $\mu_B < 1\text{GeV}$ where the pion effective theory is valid, $B_{\text{BEC}}^{\pi_\pm} > B_{\text{CSL}}^{\pi_0}$ is always satisfied. This suggests that for the parameter space of the interest, $B_{\text{CSL}}^{\pi_0} < B < B_{\text{BEC}}^{\pi_\pm}$ with $B < 1\text{GeV}^2$ and $\mu_B < 1\text{GeV}$, even the single wall disk nucleation rate, and consequently that for the CSL, is exponentially suppressed, as long as our Nambu-Goto like effective description gives a good estimate for the nucleation rate. We conclude that in order for the CSL to form quickly in the QCD system, we need a mechanism other than the topological defect formation through the quantum tunneling.

3.2 Axion Like Particle

Next we consider an axion like particle (ALP) denoted as a [40, 42, 46, 63–65], which is a pseudo Nambu-Goldstone boson associated with a global U(1) symmetry breaking and is often predicted in the low-energy effective field theory of the string compactifications [40–45]. Hence, ALPs are considered not only to be candidates of dark sector but also to show imprints of quantum gravity. It is characterized by the mass m_a , and axion decay constant f_a , which is also described by the effective potential

$$V(a) = m_a^2 f_a^2 \left(1 - \cos \frac{a}{f_a} \right), \quad (3.5)$$

with a canonical kinetic term, and the effective interactions to the SM sector,

$$\mathcal{L} \ni -\frac{g_Y^2}{32\pi^2} C_Y \frac{a}{f_a} Y_{\mu\nu} \tilde{Y}^{\mu\nu} + \sum_i \frac{X_{iR}}{f_a} (\partial_\mu a) \psi_{iR}^\dagger \sigma^\mu \psi_{iR} - \sum_j \frac{X_{jL}}{f_a} (\partial_\mu a) \psi_{jL}^\dagger \bar{\sigma}^\mu \psi_{jL}, \quad (3.6)$$

where g_Y is the hypergauge coupling constant, $Y_{\mu\nu}$ is the hypercharge gauge field strength, and ψ_{iR} and ψ_{jL} are the right- and left-handed Weyl fermions, respectively.⁶ The coefficients C_Y and $X_{iR/L}$ are determined by the UV physics. Note that the last two terms are the axion-fermion current coupling with

$$j_{iR}^\mu \equiv \psi_{iR}^\dagger \sigma^\mu \psi_{iR}, \quad j_{jL}^\mu \equiv \psi_{jL}^\dagger \bar{\sigma}^\mu \psi_{jL}. \quad (3.7)$$

Let us consider the case where the system has a uniform background hypermagnetic field \mathbf{B}_Y and the chemical potentials for each fermions, $\mu_{iR/L}$. In this case, the chiral magnetic effect induces the fermion current,

$$\mathbf{j}_{iR/L} = (-1)^{\lambda_{iR/L}} \frac{\mu_{iR/L}}{2\pi^2} (q_i g_Y) \mathbf{B}_Y, \quad (3.8)$$

where $\lambda_{iR} = 0$ and $\lambda_{iL} = 1$, respectively, and q_i is the hypercharge of the fermion ψ_i , which leads to the topological term,

$$\mathcal{L}_{\text{eff}} = \frac{g_Y}{2\pi^2} \left(\sum_i X_{iR} q_i \mu_{iR} + \sum_j X_{jL} q_j \mu_{jL} \right) \mathbf{B}_Y \cdot \nabla \left(\frac{a}{f_a} \right). \quad (3.9)$$

Then with a similar discussion in Sec. 2, we can see that the axion CSL also forms, whose properties can be read off with the replacement,

$$\phi \rightarrow \frac{a}{f_a}, \quad \mathbf{B} \rightarrow \mathbf{B}_Y, \quad \mu \rightarrow \mu_V \equiv 2g_Y \left(\sum_i X_{iR} q_i \mu_{iR} + \sum_j X_{jL} q_j \mu_{jL} \right). \quad (3.10)$$

Consequently, the same properties to the CSL formed by neutral pion in the QCD, including the formation rate, hold⁷.

The differences to the case of the CSL formed by pion in QCD are, i) we can freely take the axion mass and decay constant, ii) we do not have to worry about the tachyonic instability due to the charged pion fluctuation, and iii) the cutoff scale of the theory would be the Planck scale M_{pl} or the string scale M_{str} . In the case $m_a \ll f_a \ll M_{\text{str}}$, which is often considered in conventional models or Large Volume Scenario [41, 45, 66, 67], the critical magnetic field strength for the single domain wall formation in eq. (2.39) leads

$$B_{cY} \simeq \frac{64\pi^2 f_a^3}{\mu_V}. \quad (3.11)$$

Then we identify that for sufficiently large μ_V , the critical magnetic field strength is well below the cutoff scale squared so that it seems that the CSL can easily form. However, this gives $B_{cY} \simeq \frac{f_a}{m_a} B_{\text{DW}} \gg B_{\text{DW}} = B_{\text{CSL}}$, which makes the thin-wall approximation worse. See eqs. (2.8) and (2.42). On the other hand, if we consider a heavy ALP and take $m_a \lesssim f_a \ll M_{\text{str}}$, the critical magnetic field strength is still approximated by eq. (3.11), with being smaller than the cutoff scale, while not much larger than the critical magnetic field for the CSL $B_{cY} \gtrsim B_{\text{CSL}}$. In this case, the thin-wall approximation is relatively good.

⁶Here we do not take into account the electroweak symmetry breaking, but the same discussion applies to the system with the spontaneously broken electroweak symmetry.

⁷We have supposed that $a/f_a \rightarrow a/f_a + \theta$ under $U(1)_{\text{PQ}}$ by an appropriate choice of chiral fermion charge.

One might wonder that the ALP CSL can form in cosmology. Noting that at high temperature, $T > 10^5$ GeV, when several Yukawa interactions becomes ineffective, there are many approximate conserved charges within the SM [68–71], one can in principle have large chemical potential, $\mu_V \simeq T$, without suffering from the baryon overproduction. Then with our estimate in the above, we might expect the axion CSL formation at $T \simeq f_a \gtrsim m_a \gg 10^5$ GeV if we have strong magnetic fields $B \simeq T^2$. However, the formation rate for the CSL estimated in the above is the one at zero temperature. In order to investigate the possibility of the formation of the axion CSL in the cosmic history, we need to develop its thermal formation rate, which is left for future study.

4 Conclusion and Discussion

The ground state of the sine-Gordon theory with the background fermion chemical potential and magnetic fields, whose effect is implemented by the total derivative term (2.1) is not the vacuum state ($\phi = 0$), but the CSL state, for sufficiently large magnetic field, $B > B_{\text{CSL}}$ [6]. However, it has not been clear how the vacuum state changes to the CSL one. In this work, we tackled this problem for the first time, in the best of our knowledge, by adopting the Nambu-Goto like effective action for the string-domain wall disk system in the sine-Gordon theory with the topological term (2.1). The transition of the state from the vacuum to the CSL is described by the quantum mechanical tunneling of the radius of a domain-wall disk surrounded by a string loop from $R_d = 0$ to $R_d \neq 0$, which is a similar approach to the studies in refs. [37–39]. In this description, for $B > B_{\text{CSL}}$ the wall tension becomes negative due to the topological term. Since the effective potential of the wall-disk radius R has the potential barrier between $R = 0$ and $R \rightarrow \infty$, because of the combination of the negative wall tension and the positive string tension, a domain wall-disk with a finite radius can be formed not classically but through the quantum tunneling. In Section 2.3, we evaluated the nucleation rate of a single wall disk from the vacuum state as well as from the environment where the CSL has almost been formed, in terms of the bounce action eq. (2.37), which is the main result of the present paper. We regard that the latter represents the rate for the complete formation of the CSL. Due to the repulsive force acting between the walls, which reduces the absolute value of the wall tension, the bounce action for the disk nucleation in the environment where the CSL has almost been formed is found to be larger than that from the vacuum, and hence the nucleation rate is more suppressed. With these estimates, we determined the critical magnetic field for the disk nucleation where the exponential suppression becomes absent, $\mathcal{B} \simeq \mathcal{O}(1)$. Note that the thin-wall approximation is turned out likely to be violated for the disk with the critical radius for such large magnetic field strength. However, we expect that it gives a good estimate for the disk nucleation from the discussion in ref. [39], where the exponential suppression factor for the larger radius is turned to be equal to that for the critical radius in the case of the three-dimensional bubble nucleation. There it has been identified as the whole quantum estimate of the rate for the quantum tunneling followed by the classical expansion.

Since our analysis is based on the sine-Gordon theory with the total derivative term, the results in section 2.3 can be applied to systems described by the same Lagrangian as eq. (2.1). In section 3.1, we apply our analysis into 2-flavor QCD at finite baryon chemical potential under an external magnetic field. We found that within the scope of the low energy effective theory, the formation of a single domain-wall disk from the vacuum is exponentially suppressed, $\propto e^{-\mathcal{B}}$, $\mathcal{B} \gg 1$. Therefore, even when the CSL is more stable than the vacuum state at $B > B_{\text{CSL}}$, the vacuum state cannot be transformed into the CSL one quickly. However, there may be loopholes in the above discussion. As we have explained in the above, the thin-wall approximation for the validity of the Nambu-Goto action is not a good approximation for the disk with a critical radius, R_2 . For example, substituting

$f_\pi \approx 93 \text{ MeV}$, $m_\pi \approx 140 \text{ MeV}$ and $B = 2B_{\text{DW}}$ for eqs. (2.41) and (2.42), the ratios of the vortex size r_c as well as the wall thickness r_w to critical disk radius $R_d = R_2$ are evaluated as

$$\frac{r_c}{R_2} \sim 0.5, \quad \frac{r_w}{R_2} \sim 0.3, \quad (4.1)$$

where we have approximated the logarithmic factor to be unity. Apparently, it is not sufficiently smaller than 1. Therefore, the Nambu-Goto type effective action may not be applicable in the CSL of QCD. Note that this arguments also follows for the ALP CSL. The other potential loophole is the effects of the charged pions. We have considered the quantum nucleation of the topological soliton with the topological number $\pi_1(\text{U}(1)) \simeq \mathbb{Z}$ so far. Although the charged pions acquire masses by the Landau quantization, sufficiently heavy to be neglected, the actual configuration space of the mesons (π_0, π_\pm) is $\text{SU}(2)$ instead of $\text{U}(1)$. Hence, while we expect that the charged pions do not show nontrivial field configuration during the disk formation process due to their heavy mass, we do not exclude the possibility that the wall disk is formed continuously from the QCD vacuum due to $\pi_1(\text{SU}(2)) \simeq 0$ when we include the degrees of freedom of the charged mesons. We leave more detailed investigation in future study. Note that in the case of ALPs, which is studied in Sec. 3.2, we have considered a single ALP and it is assumed that there exist no associated light charged field in the theory. If this is the case in the string theory, loopholes would not apply. However, in general there may have to exist associated fields, e.g., lots of ALPs, in string theory owing to the swampland constraints restricting the moduli space [72, 73].

Note added: While completing this paper, we learned another study on the formation of the chiral soliton lattice [57] by M. Eto and M. Nitta.

Acknowledgements

The authors would like to thank M. Eto and M. Nitta for useful comments and for informing us of their study on the soliton formation. The authors would also like to thank M. Hongo for discussion. This work is supported by JSPS KAKENHI, Grant-in-Aid for Scientific Research (C) 22K03601 (T. H.) and JP19K03842 (K. K.). K. N. is supported by JSPS KAKENHI, Grant-in-Aid for Scientific Research (B) 21H01084.

References

- [1] I. Dzyaloshinskii, “Theory of helicoidal structures in antiferromagnets. i. nonmetals,” *Sov. Phys. JETP* **19** no. 4, (1964) 960–971.
- [2] Y. Togawa, Y. Kousaka, K. Inoue, and J.-i. Kishine, “Symmetry, structure, and dynamics of monoaxial chiral magnets,” *Journal of the Physical Society of Japan* **85** no. 11, (2016) 112001.
- [3] J.-i. Kishine and A. Ovchinnikov, “Theory of monoaxial chiral helimagnet,” *Solid State Physics* **66** (2015) 1–130.
- [4] D. T. Son and A. R. Zhitnitsky, “Quantum anomalies in dense matter,” *Phys. Rev. D* **70** (2004) 074018, [arXiv:hep-ph/0405216](#).
- [5] D. T. Son and M. A. Stephanov, “Axial anomaly and magnetism of nuclear and quark matter,” *Phys. Rev. D* **77** (2008) 014021, [arXiv:0710.1084](#) [[hep-ph](#)].
- [6] T. Brauner and N. Yamamoto, “Chiral Soliton Lattice and Charged Pion Condensation in Strong Magnetic Fields,” *JHEP* **04** (2017) 132, [arXiv:1609.05213](#) [[hep-ph](#)].

- [7] M. Eto, K. Hashimoto, and T. Hatsuda, “Ferromagnetic neutron stars: axial anomaly, dense neutron matter, and pionic wall,” [*Phys. Rev. D* **88** \(2013\) 081701](#), [arXiv:1209.4814 \[hep-ph\]](#).
- [8] M. Kawaguchi, Y.-L. Ma, and S. Matsuzaki, “Chiral soliton lattice effect on baryonic matter from a skyrmion crystal model,” [*Phys. Rev. C* **100** no. 2, \(2019\) 025207](#), [arXiv:1810.12880 \[nucl-th\]](#).
- [9] S. Chen, K. Fukushima, and Z. Qiu, “Skyrmions in a magnetic field and π^0 domain wall formation in dense nuclear matter,” [*Phys. Rev. D* **105** no. 1, \(2022\) L011502](#), [arXiv:2104.11482 \[hep-ph\]](#).
- [10] M. S. Grønli and T. Brauner, “Competition of chiral soliton lattice and Abrikosov vortex lattice in QCD with isospin chemical potential,” [*Eur. Phys. J. C* **82** no. 4, \(2022\) 354](#), [arXiv:2201.07065 \[hep-ph\]](#).
- [11] N. Yamamoto, “Axion electrodynamics and nonrelativistic photons in nuclear and quark matter,” [*Phys. Rev. D* **93** no. 8, \(2016\) 085036](#), [arXiv:1512.05668 \[hep-th\]](#).
- [12] T. Brauner and S. Kadam, “Anomalous electrodynamics of neutral pion matter in strong magnetic fields,” [*JHEP* **03** \(2017\) 015](#), [arXiv:1701.06793 \[hep-ph\]](#).
- [13] T. Brauner, H. Kolešová, and N. Yamamoto, “Chiral soliton lattice phase in warm QCD,” [*Phys. Lett. B* **823** \(2021\) 136767](#), [arXiv:2108.10044 \[hep-ph\]](#).
- [14] G. W. Evans and A. Schmitt, “Chiral anomaly induces superconducting baryon crystal,” [arXiv:2206.01227 \[hep-th\]](#).
- [15] X.-G. Huang, K. Nishimura, and N. Yamamoto, “Anomalous effects of dense matter under rotation,” [*JHEP* **02** \(2018\) 069](#), [arXiv:1711.02190 \[hep-ph\]](#).
- [16] K. Nishimura and N. Yamamoto, “Topological term, QCD anomaly, and the η' chiral soliton lattice in rotating baryonic matter,” [*JHEP* **07** no. 07, \(2020\) 196](#), [arXiv:2003.13945 \[hep-ph\]](#).
- [17] M. Eto, K. Nishimura, and M. Nitta, “Phases of rotating baryonic matter: non-Abelian chiral soliton lattices, antiferro-isospin chains, and ferri/ferromagnetic magnetization,” [arXiv:2112.01381 \[hep-ph\]](#).
- [18] H.-L. Chen, X.-G. Huang, and J. Liao, “QCD phase structure under rotation,” [*Lect. Notes Phys.* **987** \(2021\) 349–379](#), [arXiv:2108.00586 \[hep-ph\]](#).
- [19] A. Yamada and N. Yamamoto, “Floquet vacuum engineering: Laser-driven chiral soliton lattice in the QCD vacuum,” [*Phys. Rev. D* **104** no. 5, \(2021\) 054041](#), [arXiv:2107.07074 \[hep-ph\]](#).
- [20] T. Brauner, G. Filios, and H. Kolešová, “Chiral soliton lattice in QCD-like theories,” [*JHEP* **12** \(2019\) 029](#), [arXiv:1905.11409 \[hep-ph\]](#).
- [21] T. Brauner, G. Filios, and H. Kolešová, “Anomaly-Induced Inhomogeneous Phase in Quark Matter without the Sign Problem,” [*Phys. Rev. Lett.* **123** no. 1, \(2019\) 012001](#), [arXiv:1902.07522 \[hep-ph\]](#).
- [22] N. Yamamoto, “Chirality Driven Helical Pattern Formation,” [arXiv:1808.00326 \[cond-mat.stat-mech\]](#).
- [23] A. Vilenkin, “EQUILIBRIUM PARITY VIOLATING CURRENT IN A MAGNETIC FIELD,” [*Phys. Rev. D* **22** \(1980\) 3080–3084](#).
- [24] M. A. Metlitski and A. R. Zhitnitsky, “Anomalous axion interactions and topological currents in dense matter,” [*Phys. Rev. D* **72** \(2005\) 045011](#), [arXiv:hep-ph/0505072](#).
- [25] K. Fukushima, D. E. Kharzeev, and H. J. Warringa, “The Chiral Magnetic Effect,” [*Phys. Rev. D* **78** \(2008\) 074033](#), [arXiv:0808.3382 \[hep-ph\]](#).
- [26] A. Vilenkin, “MACROSCOPIC PARITY VIOLATING EFFECTS: NEUTRINO FLUXES FROM ROTATING BLACK HOLES AND IN ROTATING THERMAL RADIATION,” [*Phys. Rev. D* **20** \(1979\) 1807–1812](#).

- [27] A. Vilenkin, “QUANTUM FIELD THEORY AT FINITE TEMPERATURE IN A ROTATING SYSTEM,” [*Phys. Rev. D* **21** \(1980\) 2260–2269](#).
- [28] K. Landsteiner, E. Megias, and F. Pena-Benitez, “Gravitational Anomaly and Transport,” [*Phys. Rev. Lett.* **107** \(2011\) 021601](#), [arXiv:1103.5006 \[hep-ph\]](#).
- [29] K. Landsteiner, E. Megias, and F. Pena-Benitez, “Anomalous Transport from Kubo Formulae,” [*Lect. Notes Phys.* **871** \(2013\) 433–468](#), [arXiv:1207.5808 \[hep-th\]](#).
- [30] K. Landsteiner, “Notes on Anomaly Induced Transport,” [*Acta Phys. Polon.* **B47** \(2016\) 2617](#), [arXiv:1610.04413 \[hep-th\]](#).
- [31] D. T. Son and P. Surowka, “Hydrodynamics with Triangle Anomalies,” [*Phys. Rev. Lett.* **103** \(2009\) 191601](#), [arXiv:0906.5044 \[hep-th\]](#).
- [32] I. Dzyaloshinsky, “A thermodynamic theory of “weak” ferromagnetism of antiferromagnetics,” [*Journal of Physics and Chemistry of Solids* **4** no. 4, \(1958\) 241–255](#).
<https://www.sciencedirect.com/science/article/pii/0022369758900763>.
- [33] T. Moriya, “Anisotropic superexchange interaction and weak ferromagnetism,” [*Phys. Rev.* **120** \(Oct, 1960\) 91–98](#). <https://link.aps.org/doi/10.1103/PhysRev.120.91>.
- [34] T. W. B. Kibble, “Topology of Cosmic Domains and Strings,” [*J. Phys. A* **9** \(1976\) 1387–1398](#).
- [35] W. H. Zurek, “Cosmological Experiments in Superfluid Helium?,” [*Nature* **317** \(1985\) 505–508](#).
- [36] G. W. Paterson, T. Koyama, M. Shinozaki, Y. Masaki, F. J. Goncalves, Y. Shimamoto, T. Sogo, M. Nord, Y. Kousaka, Y. Kato, et al., “Order and disorder in the magnetization of the chiral crystal CrNb_3S_6 ,” [*Physical Review B* **99** no. 22, \(2019\) 224429](#).
- [37] R. Basu, A. H. Guth, and A. Vilenkin, “Quantum creation of topological defects during inflation,” [*Phys. Rev. D* **44** \(1991\) 340–351](#).
- [38] W.-Y. Ai and M. Drewes, “Schwinger effect and false vacuum decay as quantum-mechanical tunneling of a relativistic particle,” [*Phys. Rev. D* **102** no. 7, \(2020\) 076015](#), [arXiv:2005.14163 \[hep-th\]](#).
- [39] T. Hayashi, K. Kamada, N. Oshita, and J. Yokoyama, “Vacuum decay in the Lorentzian path integral,” [*JCAP* **05** no. 05, \(2022\) 041](#), [arXiv:2112.09284 \[hep-th\]](#).
- [40] P. Svrcek and E. Witten, “Axions In String Theory,” [*JHEP* **06** \(2006\) 051](#), [arXiv:hep-th/0605206](#).
- [41] J. P. Conlon, “The QCD axion and moduli stabilisation,” [*JHEP* **05** \(2006\) 078](#), [arXiv:hep-th/0602233](#).
- [42] A. Arvanitaki, S. Dimopoulos, S. Dubovsky, N. Kaloper, and J. March-Russell, “String Axiverse,” [*Phys. Rev. D* **81** \(2010\) 123530](#), [arXiv:0905.4720 \[hep-th\]](#).
- [43] B. S. Acharya, K. Bobkov, and P. Kumar, “An M Theory Solution to the Strong CP Problem and Constraints on the Axiverse,” [*JHEP* **11** \(2010\) 105](#), [arXiv:1004.5138 \[hep-th\]](#).
- [44] T. Higaki and T. Kobayashi, “Note on moduli stabilization, supersymmetry breaking and axiverse,” [*Phys. Rev. D* **84** \(2011\) 045021](#), [arXiv:1106.1293 \[hep-th\]](#).
- [45] M. Cicoli, M. Goodsell, and A. Ringwald, “The type IIB string axiverse and its low-energy phenomenology,” [*JHEP* **10** \(2012\) 146](#), [arXiv:1206.0819 \[hep-th\]](#).
- [46] D. J. E. Marsh, “Axion Cosmology,” [*Phys. Rept.* **643** \(2016\) 1–79](#), [arXiv:1510.07633 \[astro-ph.CO\]](#).
- [47] D. T. Son and N. Yamamoto, “Berry Curvature, Triangle Anomalies, and the Chiral Magnetic Effect in Fermi Liquids,” [*Phys. Rev. Lett.* **109** \(2012\) 181602](#), [arXiv:1203.2697 \[cond-mat.mes-hall\]](#).
- [48] K. Fukushima and S. Imaki, “Anomaly inflow on QCD axial domain-walls and vortices,” [*Phys. Rev. D* **97** no. 11, \(2018\) 114003](#), [arXiv:1802.08096 \[hep-ph\]](#).

- [49] D. B. Kaplan and S. Reddy, “Charged and superconducting vortices in dense quark matter,” [Phys. Rev. Lett.](#) **88** (2002) 132302, [arXiv:hep-ph/0109256](#).
- [50] K. B. W. Buckley and A. R. Zhitnitsky, “Superconducting K strings in high density QCD,” [JHEP](#) **08** (2002) 013, [arXiv:hep-ph/0204064](#).
- [51] Y. B. Zeldovich, I. Y. Kobzarev, and L. B. Okun, “Cosmological Consequences of the Spontaneous Breakdown of Discrete Symmetry,” [Zh. Eksp. Teor. Fiz.](#) **67** (1974) 3–11.
- [52] T. W. B. Kibble, G. Lazarides, and Q. Shafi, “Walls Bounded by Strings,” [Phys. Rev. D](#) **26** (1982) 435.
- [53] A. Vilenkin and A. E. Everett, “Cosmic Strings and Domain Walls in Models with Goldstone and PseudoGoldstone Bosons,” [Phys. Rev. Lett.](#) **48** (1982) 1867–1870.
- [54] A. Vilenkin and E. P. S. Shellard, [Cosmic Strings and Other Topological Defects](#). Cambridge University Press, 7, 2000.
- [55] M. B. Hindmarsh and T. W. B. Kibble, “Cosmic strings,” [Rept. Prog. Phys.](#) **58** (1995) 477–562, [arXiv:hep-ph/9411342](#).
- [56] C. Chatterjee, T. Higaki, and M. Nitta, “Note on a solution to domain wall problem with the Lazarides-Shafi mechanism in axion dark matter models,” [Phys. Rev. D](#) **101** no. 7, (2020) 075026, [arXiv:1903.11753 \[hep-ph\]](#).
- [57] M. Eto and M. Nitta, “Quantum nucleation of topological solitons,” [arXiv:2207.00211 \[hep-th\]](#).
- [58] S. R. Coleman, “The Fate of the False Vacuum. 1. Semiclassical Theory,” [Phys. Rev. D](#) **15** (1977) 2929–2936. [Erratum: [Phys.Rev.D](#) 16, 1248 (1977)].
- [59] C. G. Callan, Jr. and S. R. Coleman, “The Fate of the False Vacuum. 2. First Quantum Corrections,” [Phys. Rev. D](#) **16** (1977) 1762–1768.
- [60] E. J. Weinberg, [Classical solutions in quantum field theory: Solitons and Instantons in High Energy Physics](#). Cambridge Monographs on Mathematical Physics. Cambridge University Press, 9, 2012.
- [61] I. A. Shushpanov and A. V. Smilga, “Quark condensate in a magnetic field,” [Phys. Lett. B](#) **402** (1997) 351–358, [arXiv:hep-ph/9703201](#).
- [62] N. O. Agasian and I. A. Shushpanov, “The Quark and gluon condensates and low-energy QCD theorems in a magnetic field,” [Phys. Lett. B](#) **472** (2000) 143–149, [arXiv:hep-ph/9911254](#).
- [63] J. Preskill, M. B. Wise, and F. Wilczek, “Cosmology of the Invisible Axion,” [Phys. Lett. B](#) **120** (1983) 127–132.
- [64] L. F. Abbott and P. Sikivie, “A Cosmological Bound on the Invisible Axion,” [Phys. Lett. B](#) **120** (1983) 133–136.
- [65] M. Dine and W. Fischler, “The Not So Harmless Axion,” [Phys. Lett. B](#) **120** (1983) 137–141.
- [66] V. Balasubramanian, P. Berglund, J. P. Conlon, and F. Quevedo, “Systematics of moduli stabilisation in Calabi-Yau flux compactifications,” [JHEP](#) **03** (2005) 007, [arXiv:hep-th/0502058](#).
- [67] J. P. Conlon, F. Quevedo, and K. Suruliz, “Large-volume flux compactifications: Moduli spectrum and D3/D7 soft supersymmetry breaking,” [JHEP](#) **08** (2005) 007, [arXiv:hep-th/0505076](#).
- [68] B. A. Campbell, S. Davidson, J. R. Ellis, and K. A. Olive, “On the baryon, lepton flavor and right-handed electron asymmetries of the universe,” [Phys. Lett. B](#) **297** (1992) 118–124, [arXiv:hep-ph/9302221](#).
- [69] B. Garbrecht and P. Schwaller, “Spectator Effects during Leptogenesis in the Strong Washout Regime,” [JCAP](#) **10** (2014) 012, [arXiv:1404.2915 \[hep-ph\]](#).

- [70] V. Domcke, Y. Ema, K. Mukaida, and M. Yamada, “Spontaneous Baryogenesis from Axions with Generic Couplings,” [JHEP](#) **08** (2020) 096, [arXiv:2006.03148 \[hep-ph\]](#).
- [71] V. Domcke, K. Kamada, K. Mukaida, K. Schmitz, and M. Yamada, “Wash-In Leptogenesis,” [Phys. Rev. Lett.](#) **126** no. 20, (2021) 201802, [arXiv:2011.09347 \[hep-ph\]](#).
- [72] C. Vafa, “The String landscape and the swampland,” [arXiv:hep-th/0509212](#).
- [73] E. Palti, “The Swampland: Introduction and Review,” [Fortsch. Phys.](#) **67** no. 6, (2019) 1900037, [arXiv:1903.06239 \[hep-th\]](#).